Title

A CK1α Activator Penetrates the Brain and Shows Efficacy Against Drug-resistant Metastatic Medulloblastoma

Journal

Clinical Cancer Research, 25(4)

ISSN

1078-0432

Authors

Rodriguez-Blanco, Jezabel
Li, Bin
Long, Jun
et al.

Publication Date

2019-02-15

DOI

10.1158/1078-0432.ccr-18-1319

Peer reviewed

A CK1α Activator Penetrates the Brain and Shows Efficacy Against Drug-resistant Metastatic Medulloblastoma

Jezabel Rodriguez-Blanco[1], Bin Li[1], Jun Long[1], Chen Shen[1], Darren Orton[2], Sara Collins[3], Noriyuki Kasahara[3,6], Mehrdad Nadji[4], Nagi G. Ayad[5,6], Martine Roussel[7], William A. Weiss[8], Anthony J. Capobianco[1,6], David J. Robbins[1,6*]

[1]Molecular Oncology Program, The DeWitt Daughtry Family Department of Surgery, University of Miami, Miller School of Medicine, Miami, FL.
[2]StemSynergy Therapeutics Inc., Miami FL.
[3]Department of Cell Biology, University of Miami, Miller School of Medicine, Miami, FL.
[4]Department of Pathology, University of Miami. Miller School of Medicine, Miami, FL.
[5]Center for Therapeutic Innovation, Department of Psychiatry and Behavioral Sciences, University of Miami, Miller School of Medicine, Miami, FL.
[6]Sylvester Comprehensive Cancer Center, University of Miami, FL.
[7]Department of Tumor Cell Biology, St Jude Children's Research Hospital (SJCRH), Memphis, TN.
[8]Department of Neurobiology, University of California, San Francisco, CA.

*Corresponding author:
David J. Robbins, PhD
Molecular Oncology Program,
The DeWitt Daughtry Family Department of Surgery,
University of Miami Miller School of Medicine
1600 NW 10th Avenue, Miami, FL 33136, USA
email: drobbins@miami.edu
Phone: 305-243-5717

Running Title: CK1α activators attenuate growth of SMO inhibitor resistant medulloblastoma

Key Words: SONIC HEDGEHOG, Medulloblastoma, CK1α, therapy, SSTC3

Abstract

Purpose: Although most children with medulloblastoma are cured of their disease, Sonic Hedgehog (SHH) subgroup medulloblastoma driven by TRP53 mutations is essentially lethal. Casein kinase 1α (CK1α) phosphorylates and destabilizes GLI transcription factors, thereby inhibiting the key effectors of SHH signaling. We therefore tested a second-generation CK1α activator against TRP53-mutant, MYCN-amplified medulloblastoma.

Experimental Design: The ability of this CK1α activator to block SHH signaling was determined in vitro using GLI reporter cells, granular precursor primary cultures, and PATCHED1 (PTCH1)-mutant sphere cultures. While in vivo efficacy was tested using 2 different medulloblastoma mouse models: PTCH1 and ND2:SMOA1. Finally, the clinical relevance of CK1α activators was demonstrated using a TRP53-mutant, MYCN-amplified patient-derived xenograft.

Results: SSTC3 inhibited SHH activity in vitro, acting downstream of the vismodegib target SMOOTHENED (SMO), and reduced the viability of sphere cultures derived from SHH medulloblastoma. SSTC3 accumulated in the brain, inhibited growth of SHH medulloblastoma tumors, and blocked metastases in a genetically engineered vismodegib-resistant mouse model of SHH medulloblastoma. Importantly, SSTC3 attenuated growth and metastasis of orthotopic patient-derived TRP53-mutant, MYCN-amplified, SHH subgroup medulloblastoma xenografts, increasing overall survival.

Conclusions: Using a newly described small-molecule, SSTC3, we show that CK1a activators could address a significant unmet clinical need for patients with SMO inhibitor–resistant medulloblastoma, including those harboring mutations in TRP53.

Introduction

Medulloblastoma (MB) is the most common pediatric brain tumor, for which the standard of care is typically surgery followed by radiation and/or chemotherapy*(1)*. Comprehensive genomic and bioinformatic analysis has allowed MB to be stratified into four major subgroups, with distinct molecular drivers and prognoses*(2, 3)*. This genomic stratification of MB is being used to guide the development of novel subgroup specific targeted therapies*(4)*. Approximately one-third of MB patients harbor tumors associated with constitutive SONIC HEDGEHOG activity (SHH subgroup)*(5)*. Although the five-year survival of SHH subgroup patients is reasonably high, a subset of these patients, which harbor *TRP53* mutations and *MYCN* amplification, display resistance to standard of care therapy*(6–8)*. As few additional therapeutic options are available for this cohort of patients they exhibit a significantly reduced five-year survival rate.

SHH signaling is initiated upon its family of ligands binding to their receptor PATCHED1 (PTCH1) or loss of function mutations in *PTCH1(9)*, the latter of which is the major molecular driver for SHH subgroup MB*(10)*. Either of these mechanisms results in the derepression of the seven-transmembrane protein SMOOTHENED (SMO). Ultimately, SMO regulates a signaling pathway that results in the stabilization and activation of the GLI family of transcription factors*(11)*, in a manner that involves reduced phosphorylation of GLI proteins by PKA and CK1α*(12–14)*. Suppressor of fused (SUFU) acts to repress GLI activation and this repression is overcome via trafficking through primary cilia, in a manner downstream of SMO*(15)*.

A number of small-molecule SMO inhibitors have been evaluated in the clinic. One of these inhibitors, vismodegib, was FDA approved for the treatment of advanced basal cell carcinoma (BCC)*(16)*. Although vismodegib showed dramatic efficacy against BCC, a number of patients relapsed due to selection for mutations at or downstream of *SMO(17)*. However, given its efficacy against BCC driven by constitutive SHH activity, vismodegib was rapidly repurposed in clinical trials for MB patients*(18)*. Vismodegib also exhibited efficacy against SHH subgroup MB patients,

but predominantly for those patients whose cancer is driven by *PTCH1* mutations*(19)*. However, even with the limited number of patients treated with vismodegib, rapid tumor recurrence has already been observed in the clinic, likely driven by mutations in or downstream of *SMO(20)*. These examples with the first-in-class SMO inhibitor vismodegib illustrate the clinical potential of SMO inhibitors for MB patients, as well as the importance of developing and clinically evaluating SHH inhibitors that act downstream of SMO.

We previously described a first-in-class CK1α activator, pyrvinium, which acts as a potent inhibitor of SHH signaling downstream of SMO, via the phosphorylation and destabilization of GLI1 and GLI2*(21)*. Although we showed that pyrvinium was able to reduce the growth of SHH subgroup MB *in vivo*, its poor bioavailability limited this demonstration of efficacy to MB implanted in the flanks of mice and dosed by local administration of pyrvinium. We recently described a second-generation CK1α activator with significantly improved pharmacokinetics, SSTC3*(22)*. We now show the ability of SSTC3 to inhibit SHH signaling *in vitro* and *in vivo*. We take advantage of the improved pharmacokinetics of SSTC3, demonstrating its ability to cross the blood brain barrier, attenuate the growth of SHH subgroup MB mouse models, and prolong their survival. Most importantly, we also demonstrate the efficacy of SSTC3 against orthotopically implanted, patient derived *TRP53* mutant MB, one of the most clinically challenging forms of MB*(6, 23, 24)*.

Methods and Materials

Cell and molecular biology

NIH-3T3 and HEK293T cells were purchased from American Type Culture Collection (ATCC) and cultured as recommended by ATCC. The efficacy of SSTC was validated using LIGHT2 cells, a cell line derived from NIH-3T3 cells stably expressing a GLI-dependent firefly luciferase reporter gene and a constitutive *Renilla* luciferase reporter gene, in presence of 0.1% new born calf serum. GLI driven firefly luciferase activity was normalized to the *Renilla* luciferase control, and Luciferase activity determined using a dual luciferase kit (Promega)*(25)*. SUFU$^{-/-}$ MEFs were a

gift of Dr. Toftgard and were cultured in DMEM and 10% fetal bovine serum. Medulloblastoma sphere cultures (MBSC) were obtained by digesting MB tissue for 10 minutes using Accutase (Invitrogen) at 37°C and sequentially selecting single cell suspensions using 100 µm and 70 µm cell strainers (BD). The resulting cell suspensions were grown *ex vivo* in DMEM/F12, 2% B27 and Pen-Strep (Invitrogen), and allowed to form spheres for up to 10 days. MBSC were maintained in culture for a maximum of 10 passages*(26)*. For analysis by indirect immunofluorescence the MBSCs were plated on chamber slides (Millipore) previously coated with poly-L-ornithine/laminin (Sigma). The isolation and culture of granular precursor cells (GPC) from P4-6 C57BL/6 mice was performed using the Papain Dissociation System (Worthington). Cells were plated on poly-L-lysine coated plates in Neurobasal-A, 1% Glutamax, 2% B27 and 250 µM KCl*(27)*. Plasmids expressing *GLI1*, a gift of Dr. Oro (Stanford), wild type *SMO* (Addgene), or the *SMO D473M2* double mutant (Addgene), were transfected into cells using Lipofectamine 2000 (Invitrogen). All lentiviral shRNA constructs are in the *pLKO.1* vector (Dharmacon), and the subsequent lentivirus packaged and transduced into cells as previously described*(28)*. shRNA expressing LIGHT2 cells were selected by 10 µg/ml puromycin.

For gene expression analyses total RNA was Trizol (Invitrogen) extracted, converted into cDNA (Applied Biosystems) and analyzed using quantitative real-time PCR (RT-qPCR) and Taqman probes (Invitrogen). *GAPDH* expression was used for normalization. RIPA buffer (Thermo) was used for protein extraction and levels of the indicated proteins determined by immunoblotting using antibodies purchased from Cell Signaling. Cell proliferation was determined using a BrdU assay, in which BrdU (10 µM) was added to cells 2 hours prior to fixation and staining*(28)*. Reduction of 3-(4,5-dimethyl-2-thiazolyl) 2,5-diphenyl-2H-tetrazolium bromide (MTT) to formazan was used to determine cell viability*(29)*. SSTC3 abundance in plasma and brain tissue was determined following protein precipitation, methanol extraction, analyses by LC/MS/MS and comparison to a corresponding calibration curve. After separation on a C18 reverse phase HPLC column (Agilent) using an acetonitrile-water gradient system, peaks were analyzed by MS using

ESI ionization in multiple reaction monitoring mode. LC/MS/MS was performed using an Agilent 6410 mass spectrometer coupled with an Agilent 1200 HPLC and a CTC PAL chilled autosampler, controlled by MassHunter software (Agilent).

Animal studies

All animal studies were conducted in accordance with protocols approved by the Institutional Animal Care and Use Committee at the University of Miami. *PTCH1* (*PTCH1*^{TM1MPS}*/J(30)*) or *ND2:SMOA1* (C57BL/6-Tg(NEUROD2-SMO*A1)199JOLS/J) mice (Jackson laboratory) were mated to generate breeding colonies. Spontaneous tumors from *PTCH1*$^{+/-}$ mice were expanded and maintained in 6-week old male *CD1-Foxn1*^{nu} mice as allografts (Charles River Laboratories). A similar protocol was used to expand a *TRP53* mutant, *MYCN* amplified patient derived xenograft (PDX) (TB-14-7196). For orthotopic implantation 10,000 *PTCH1*$^{+/-}$ mouse MB cells or 1,000,000 *TRP53* mutant, *MYCN* amplified human MB cells were resuspended in 3 µl serum free media and implanted into the cerebellum of 6-week old male *CD1-Foxn1*^{nu} mice. Coordinates used were 2 mm down lambda, 2 mm right of the middle line suture, 2 mm deep*(31)*. SSTC3 (StemSynergy Therapeutics Inc.) was diluted in DMSO to a final volume of 50 µl and administrated via intraperitoneal injection. The number of tumor lesions, defined as the number of *in situ* tumors plus local metastasis found per slide, were quantified to determine the total tumor burden. For immunohistochemistry analyses mouse tissues were fixed in 10% formalin for 48 hours prior to staining with the indicated antibodies, following the manufacturer's recommendations (Cell Signaling). A TACS® TdT *in situ* DAB kit (R&D Systems) for TERMINAL DEOXYNUCLEOTIDYL TRANSFERASE (TdT) dUTP Nick-End Labeling (TUNEL) was used to detect DNA fragmentation, following the manufacturers recommendations. Tumor area was quantified using H&E stained slides imaged using an Olympus IX7I microscope, and measured using CellSens software (Olympus). In symptom-free survival experiments, mice were sacrificed upon developing MB symptoms (such as hunch position, characteristic circling, hemineglect or ataxia) or 9 months

after treatment withdrawal for *ND2:SMOA1* mice (90 days for *TRP53* mutant, *MYCN* amplified PDX).

In vivo tumor detection in *ND2:SMOA1* mice was determined after intravenous injection of AngioSense 680 EX and 750 EX (Perkin Elmer). For luciferase imaging of *TRP53* mutant, *MYCN* amplified tumors, resected tumor cells were centrifuged in the presence of luciferase expressing lentivirus at 2000 rpm for 2 hours at 4 °C prior to implantation. D-Luciferin (Perkin Elmer) was administrated intraperitoneally to each mouse (150 mg/kg) 10 minutes before imaging. All tumor imaging was performed using a Caliper/Xenogen IVIS® SPECTRUM. Luciferase intensity was determined by measuring luminescence signal in the brain using Living Image® advanced *in vivo* imaging software (Perkin Elmer).

Statistical analysis

Results shown from *in vitro* analyses represent the mean of at least three independent experiments +/- SEM. For BrdU staining 4 fields per condition, from 3 independent experiments, were quantified. For IHC quantification, the results shown represent the mean and SEM of at least 4 fields from 3 different mice. At least 5 mice per experimental condition were used for RNA and 4 for protein analyses. For tumor size studies the results shown represent the mean and SEM of at least 12 mice per experimental condition. Significance for two sample analyses was determined using an unpaired Student's t-test. In multiple group comparisons, significance was determined using a one-way analysis of variance (ANOVA) followed by a post-hoc Student-Newman-Keuls analysis. For survival analyses at least 10 mice per experimental condition were used and significance calculated using a Log-rank (Mantel-Cox) test. Statistical significance was reached when $p < 0.05$.

Results

The second-generation CK1α activator SSTC3 attenuated the activity of a commonly used SHH-dependent reporter gene assay (EC_{50} 68 nM), relative to its inactive structural analog SSTC111 (Figure 1A). SSTC3 was also able to reduce the expression of a known SHH target gene (*GLI1*) in a time and dose dependent manner (Figure 1B), and this attenuation of *GLI1* expression occurred in a CK1α dependent manner (Figure 1C & Supplemental 1). To further determine the ability of SSTC3 to attenuate SHH signaling we also utilized primary GPC, whose proliferation is dependent on SHH activity. SSTC3 attenuated the SMO agonist (SAG) driven proliferation of GPC (Figure 1D & E) in an on-target manner, as it also attenuated the expression of SHH target genes (Figure 1F). Consistent with SSTC3 acting downstream of SMO, it was able to attenuate SHH activity driven by two clinically relevant, vismodegib resistant drivers of MB: loss of *SUFU* and a constitutive active form of SMO engineered to be vismodegib resistant (*SMOM2:D473*) (Figure 1G & H). Additionally, when new protein synthesis was blocked, SSTC3 treatment of NIH-3T3 cells resulted in decreased stability of GLI1 protein, a known CK1α target (Figure 1I). Thus, SSTC3 is able to attenuate SHH activity in a manner similar to that previously described for the first-in-class CK1α activator pyrvinium*(21)*, acting downstream of SMO to regulate GLI stability.

A number of groups have isolated and characterized MBSC from SHH subgroup MB*(32–37)*, the majority of which become insensitive to SMO antagonists*(38)*. The Segal group recently described a novel culturing system that allows MBSC to retain their sensitivity to SMO antagonists*(26)*. We isolated sphere cultures from *PTCH1* mutant driven MB using these culturing conditions and validated them, showing that their viability and expression of two SHH target genes was sensitive to low doses of vismodegib (Figure 2A & Supplemental 2A). *SMO* knockdown also reduced the viability of the MBSC and reduced the expression of *GLI1* (Figure 2B & 2C), relative to a control shRNA. We next treated these characterized MBSC with SSTC3 or SSTC111, and showed that SSTC3 attenuated their viability in a potent, dose-dependent manner relative to SST111 treatment (Figure 2D). SSTC3 also attenuated the expression of SHH target genes in these MBSC, and did in a dose dependent manner (Figure 2E). The decrease in MBSC viability

we observe upon SSTC3 treatment is likely due to decreased proliferation, as we observe a decrease in BrdU incorporation upon SSTC3 exposure (Figure 2F).

One of the challenges of treating brain tumors with drugs is their variable ability to penetrate the blood brain barrier (BBB). We show that SSTC3 is BBB penetrant, enriching in the brain to levels comparable to those found in serum (Figure Supplemental 2B). This is in stark contrast to pyrvinium, whose levels in the serum are essentially undetectable*(39)*. Taking advantage of this enrichment of SSTC3 in the brain, we treated mice with orthotopic *PTCH1* MB implants with SSTC3 for 30 days. The SSTC3 exposed residual tumors were significantly smaller than vehicle treated tumors (Figure 2G & Supplemental 2C). Furthermore, we also observed reduced proliferation (Figure 2H & 2I) and increased apoptosis (Figure 2J & 2K) of the MB cells *in vivo*. Consistent with SSTC3 acting on target *in vivo*, SSTC3 exposed tissue exhibited a reduction in SHH target genes (Figure Supplemental 2D) and decreased levels of GLI1 protein (Figure Supplemental 2E & F). Thus, SSTC3 is BBB penetrant and exhibits efficacy against a *PTCH1* mutant driven orthotopic MB mouse model.

We next tested the efficacy of SSTC3 in a genetically engineered mouse model (GEM) of MB, driven by a vismodegib insensitive oncogenic *SMO* mutant (*SMOA1*)*(40–43)*. We treated a cohort of 8-week-old *ND2:SMOA1* mice with SSTC3, or vehicle, and determined tumor growth by IVIS imaging (Figure 3A), pathologically (Figure 3B-C), or by measuring tumor area (Figure 3D). In all cases, SSTC3 exhibited dramatic effects on MB growth. Importantly, quantification of local metastases in these mice, which are commonly observed in this GEM*(40)*, also showed a significant reduction in the SSTC3 treated group (Figure 3E). Further, SSTC3 treated tumors exhibited decreased proliferation (Figure 3F-G) and increased apoptosis (Figure 3H & I, & Supplemental 3A & B). Consistent with SSTC3 attenuating tumor growth in an on-target manner, MB tissue exposed to SSTC3 exhibited decreased expression of SHH target genes (Figure 3J). Given the dramatic effects of SSTC3 on acute MB growth, we next examined the effects of SSTC3

treatment on MB symptom-free survival. We therefore treated a cohort of 8-week-old *ND2:SMOA1* mice with SSTC3 for one month and then monitored their symptom-free survival. Even with this limited exposure to SSTC3 we observed a significant increase in symptom-free survival in mice exposed to SSTC3 (Figure 3K), with 40% percent of the SSTC3 mice still symptom-free 9 months after treatment withdrawal.

In a recent clinical trial, vismodegib exhibited poor efficacy against *TRP53* mutant SHH subgroup MB patients*(19)*, likely due to *GLI* amplifications driving non-canonical SHH signaling downstream of SMO. As SSTC3 acts downstream of SMO, we hypothesized that it would exhibit efficacy against this most clinically challenging form of MB. Mice carrying such a PDX developed MB symptoms within 5 weeks, including hydrocephalus with fontanelle bulging, head tilt, hunched posture, and ataxia. Similar to the histology reported for primary *MYCN* amplified*(44)*, *TRP53* SHH subgroup MB samples, these PDX displayed large cell histology that was highly invasive (Figure Supplemental 4A). Three weeks after tumor implantation we treated this cohort of mice with vehicle or SSTC3 for two days and then harvested MB tissue. SSTC3 attenuated the expression of a subset of human specific *GLI* driven target genes in these PDXs, relative to vehicle treated mice (Figure 4A). This result suggests that SSTC3 can reduce GLI signaling in human SHH subgroup MB tissue known to be vismodegib resistant in the clinic. Cells derived from this PDX were infected with a luciferase expressing virus and orthotopically implanted into immunocompromised mice. After three days of implantation the mice were treated with vehicle or SSTC3 and tumor size monitored 7 days later. SSTC3 exposure significantly reduced the size of the tumors in these mice (Figure 4B & Supplemental 4B). Similar results were obtained when this PDX was orthotopically implanted into immnuocompromised mice and chronically treated with vehicle or SSTC3 (Figure 4C & D). Consistent with this reduction in tumor size, MB tissue similarly exposed to SSTC3 showed reduced proliferation (Figure 5E & F) and increased levels of apoptotic biomarkers relative to vehicle treated mice (Figure 4G & H, Supplemental 4C & D). A larger cohort of mice was also treated with SSTC3 for 30 days, and then monitored for symptom-free survival.

SSTC3 treated mice exhibited a significant increase in symptom-free survival over vehicle treated mice (35 days median survival for the vehicle treated mice *versus* 57 days for the SSTC3 ones) (Figure 4I).

Discussion

We show that a novel small-molecule CK1α activator, SSTC3, acts to attenuate GLI signaling, and does so in a CK1α dependent manner. SSTC3 inhibits SHH signaling downstream of SMO *in vitro* and *in vivo,* bypassing mechanisms of SMO inhibitor resistance commonly observed in the clinic*(17, 43, 45)*. Further, unlike the first-in-class CK1α activator pyrvinium*(46)*, SSTC3 enriches in serum and crosses the BBB to attenuate SHH signaling, reduce tumor growth, and increase the survival of two distinct mouse models of SHH subgroup MB. One of these mouse models of MB (*ND2:SMOA1*) exhibits numerous pathological markers of local metastases, including leptomeningeal spread*(40)*, which is uniformly lethal in MB patients*(47, 48)*. Significantly, SSTC3 was also able to reduce the emergence of these pathological markers of MB metastasis. Thus, CK1α activators represent a BBB permeable, small-molecule GLI inhibitor with the potential to target SHH subgroup MB patients, including those that exhibit local metastasis.

The discovery of the natural product cyclopamine as the first-in-class SMO antagonist *(49)*prompted the screening and preclinical development of SMO inhibitors with improved pharmacokinetic properties. Two such SMO inhibitors, vismodegib and sonidegib, are currently FDA approved for use in advanced basal cell carcinoma patients[10,42,43], and a number of others are in various stages of clinical trials*(50)*. Although exhibiting dramatic initial efficacy, recurrent BCC due to vismodegib resistance is commonly observed[44]. Deep sequencing of relapsed BCC tissue identified mutations in *SMO* as a common mechanism of such drug resistance, and also identified mutations in several genes that act downstream of *SMO*- such as *GLI* amplifications and loss of function mutations in *SUFU(17, 51)*. The promising results observed in advanced BCC patients resulted in the rapid repurposing of vismodegib for MB

patients. Vismodegib exhibited significant efficacy in SHH subgroup MB patients, although rapid tumor recurrence was also commonly observed in these patients*(20)*. These mechanisms of vismodegib resistance underscore the clinical need for novel targeted therapies that act downstream of SMO, especially those that act on GLI proteins themselves. Consistent with transcription factors being difficult to target in the clinic, only a handful of such inhibitors have been described*(53)*. One of these, arsenic trioxide (ATO), binds directly to the zinc finger region of GLI proteins to inhibit their activity*(54)*. As ATO is already FDA approved, for a subtype of leukemia*(55)*, clinical trials repurposing it as a GLI inhibitor have already being performed for advanced BCC patients (NCT01791894). Unfortunately, the micromolar potency and limited BBB permeability of ATO*(56)* is likely to limit its clinical utility for MB patients. The family of bromodomain and extraterminal domain (BET) inhibitors has also been shown to attenuate GLI activity, binding to and inhibiting the transcription of *GLI1* and *GLI2(57–59)*. One of these small-molecules, OTX015, has been shown to be BBB permeable and is currently being evaluated in clinical trials for glioblastoma (NCT02296476).

Most importantly, our work shows that SSTC3 exhibits efficacy against patient derived *TRP53* mutant, *MYCN* amplified SHH MB, a form of SHH subgroup MB that remains clinically refractory*(24)*. *TRP53* mutations are present in approximately 30% of childhood SHH MB, both as somatic and germ line mutations (Li-Fraumeni syndrome), and are considered the most important risk factor for SHH subgroup MB patients*(6, 23, 24)*. Clinical trials of vismodegib in MB patients showed no benefit for this subset of SHH subgroup patients*(19)*, likely due to the downstream amplifications of *GLI* and *MYCN* commonly associated with *TRP53* mutation in MB*(60)*. Thus, CK1α agonists represent a novel class of therapeutic capable of bypassing the common mechanisms that underlie SMO inhibitor resistance in the clinic, and which exhibits significant promise for treating this subset of SHH subgroup MB patients who have few therapeutic options.

We have previously shown that a subset of SHH subgroup MB initiating cells are actually WNT dependent, and that inhibition of WNT signaling attenuates MB growth*(31)*. We have also shown that CK1α activators can function as WNT inhibitors *in vitro* and *in vivo(22, 46, 61)*. We therefore examined the expression of two commonly used WNT biomarkers in our various MB tissues, to rule out that SSTC3 was attenuating MB growth via a reduction in WNT activity. We did not observe significant changes in WNT target gene expression upon SSTC3 exposure, consistent with SSTC3 acting as a GLI inhibitor in these mouse models of MB which do not have a significant WNT signature*(21)* (Supplemental 2G and 3C). However, consistent with our previous mouse *PTCH1*;*TRP53* mutant MB models, *TRP53* mutant PDXs exhibited significant WNT target gene expression and this expression could be reduced upon exposure to SSTC3 (Supplemental 4E). Thus, although SSTC3 exhibits significant efficacy in reducing the growth of *TRP53* mutant MB PDX, we are unable to determine if a subset of this activity is a result of attenuating WNT driven tumor-initiating cells. Regardless of the exact mechanism of action, we present here evidence for a novel BBB penetrant, small-molecule CK1α activator that is capable of attenuating the growth of a clinically refractory form of MB.

Acknowledgements

We would like to thank members of the Robbins, Capobianco and Ayad laboratories for providing their insights during discussions regarding this manuscript. **Funding**: Alex Lemonade Stand Foundation M1201547 (DJR), 1R21NS096502-01 (DJR), B*Cured (DJR), Childhood Brain Tumor Foundation (JRB), FICYT POST10-27 (JRB), and funds from the Sylvester Comprehensive Cancer Center (JRB, DJR). **Author contributions**: DJR, BL and JRB conceived and designed the experiments. JRB, BL, JL, CS and DO performed the experiments and contributed to mouse work. JRB and DJR analyzed data. SC, MR, NK and NA contributed reagents/materials/analytic tools. MR, NA, WAW and AJC gave technical support and conceptual advice. MN provided pathological insights. DJR and JRB wrote the paper. **Competing Interests**: DJR, AJC, WAW are

founders of StemSynergy Therapeutics Inc., a company focused on commercializing small molecule signaling inhibitors, such as SSTC3. D.O. is an employee of StemSynergy Therapeutics.

References:

1. R. J. Packer, P. Cogen, G. Vezina, L. B. Rorke, Medulloblastoma: clinical and biologic aspects, *Neuro. Oncol.* **1**, 232–250 (1999).

2. D. N. Louis, H. Ohgaki, O. D. Wiestler, W. K. Cavenee, P. C. Burger, A. Jouvet, B. W. Scheithauer, P. Kleihues, The 2007 WHO classification of tumours of the central nervous system, *Acta Neuropathol.* **114**, 97–109 (2007).

3. M. D. Taylor, P. A. Northcott, A. Korshunov, M. Remke, Y.-J. Cho, S. C. Clifford, C. G. Eberhart, D. W. Parsons, S. Rutkowski, A. Gajjar, D. W. Ellison, P. Lichter, R. J. Gilbertson, S. L. Pomeroy, M. Kool, S. M. Pfister, Molecular subgroups of medulloblastoma: the current consensus., *Acta Neuropathol.* **123**, 465–72 (2012).

4. B. L. Holgado, A. Guerreiro Stucklin, L. Garzia, C. Daniels, M. D. Taylor, Tailoring Medulloblastoma Treatment Through Genomics: Making a Change, One Subgroup at a Time., *Annu. Rev. Genomics Hum. Genet.* **18**, 143–166 (2017).

5. D. N. Louis, A. Perry, P. Burger, D. W. Ellison, G. Reifenberger, A. von Deimling, K. Aldape, D. Brat, V. P. Collins, C. Eberhart, D. Figarella-Branger, G. N. Fuller, F. Giangaspero, C. Giannini, C. Hawkins, P. Kleihues, A. Korshunov, J. M. Kros, M. Beatriz Lopes, H.-K. Ng, H. Ohgaki, W. Paulus, T. Pietsch, M. Rosenblum, E. Rushing, F. Soylemezoglu, O. Wiestler, P. Wesseling, International Society Of Neuropathology--Haarlem consensus guidelines for nervous system tumor classification and grading, *Brain Pathol.* **24**, 429–435 (2014).

6. U. Tabori, B. Baskin, M. Shago, N. Alon, M. D. Taylor, P. N. Ray, E. Bouffet, D. Malkin, C. Hawkins, Universal poor survival in children with medulloblastoma harboring somatic TP53 mutations., *J. Clin. Oncol.* **28**, 1345–50 (2010).

7. F. M. G. Cavalli, M. Remke, L. Rampasek, J. Peacock, D. J. H. Shih, B. Luu, L. Garzia, J. Torchia, C. Nor, A. S. Morrissy, S. Agnihotri, Y. Y. Thompson, C. M. Kuzan-Fischer, H. Farooq,

K. Isaev, C. Daniels, B.-K. Cho, S.-K. Kim, K.-C. Wang, J. Y. Lee, W. A. Grajkowska, M. Perek-Polnik, A. Vasiljevic, C. Faure-Conter, A. Jouvet, C. Giannini, A. A. Nageswara Rao, K. K. W. Li, H.-K. Ng, C. G. Eberhart, I. F. Pollack, R. L. Hamilton, G. Y. Gillespie, J. M. Olson, S. Leary, W. A. Weiss, B. Lach, L. B. Chambless, R. C. Thompson, M. K. Cooper, R. Vibhakar, P. Hauser, M.-L. C. van Veelen, J. M. Kros, P. J. French, Y. S. Ra, T. Kumabe, E. López-Aguilar, K. Zitterbart, J. Sterba, G. Finocchiaro, M. Massimino, E. G. Van Meir, S. Osuka, T. Shofuda, A. Klekner, M. Zollo, J. R. Leonard, J. B. Rubin, N. Jabado, S. Albrecht, J. Mora, T. E. Van Meter, S. Jung, A. S. Moore, A. R. Hallahan, J. A. Chan, D. P. C. Tirapelli, C. G. Carlotti, M. Fouladi, J. Pimentel, C. C. Faria, A. G. Saad, L. Massimi, L. M. Liau, H. Wheeler, H. Nakamura, S. K. Elbabaa, M. Perezpeña-Diazconti, F. Chico Ponce de León, S. Robinson, M. Zapotocky, A. Lassaletta, A. Huang, C. E. Hawkins, U. Tabori, E. Bouffet, U. Bartels, P. B. Dirks, J. T. Rutka, G. D. Bader, J. Reimand, A. Goldenberg, V. Ramaswamy, M. D. Taylor, Intertumoral Heterogeneity within Medulloblastoma Subgroups., *Cancer Cell* **31**, 737–754.e6 (2017).

8. E. C. Schwalbe, J. C. Lindsey, S. Nakjang, S. Crosier, A. J. Smith, D. Hicks, G. Rafiee, R. M. Hill, A. Iliasova, T. Stone, B. Pizer, A. Michalski, A. Joshi, S. B. Wharton, T. S. Jacques, S. Bailey, D. Williamson, S. C. Clifford, Novel molecular subgroups for clinical classification and outcome prediction in childhood medulloblastoma: a cohort study., *Lancet. Oncol.* **18**, 958–971 (2017).

9. D. J. Robbins, D. L. Fei, N. A. Riobo, The Hedgehog signal transduction network., *Sci. Signal.* **5**, re6 (2012).

10. M. Kool, D. T. W. Jones, N. Jäger, P. A. Northcott, T. J. Pugh, V. Hovestadt, R. M. Piro, L. A. Esparza, S. L. Markant, M. Remke, T. Milde, F. Bourdeaut, M. Ryzhova, D. Sturm, E. Pfaff, S. Stark, S. Hutter, H. Seker-Cin, P. Johann, S. Bender, C. Schmidt, T. Rausch, D. Shih, J. Reimand, L. Sieber, A. Wittmann, L. Linke, H. Witt, U. D. Weber, M. Zapatka, R. König, R. Beroukhim, G. Bergthold, P. van Sluis, R. Volckmann, J. Koster, R. Versteeg, S. Schmidt, S. Wolf, C. Lawerenz, C. C. Bartholomae, C. von Kalle, A. Unterberg, C. Herold-Mende, S. Hofer, A. E. Kulozik, A. von Deimling, W. Scheurlen, J. Felsberg, G. Reifenberger, M. Hasselblatt, J. R.

Crawford, G. A. Grant, N. Jabado, A. Perry, C. Cowdrey, S. Croul, G. Zadeh, J. O. Korbel, F. Doz, O. Delattre, G. D. Bader, M. G. McCabe, V. P. Collins, M. W. Kieran, Y.-J. Cho, S. L. Pomeroy, O. Witt, B. Brors, M. D. Taylor, U. Schüller, A. Korshunov, R. Eils, R. J. Wechsler-Reya, P. Lichter, S. M. Pfister, ICGC PedBrain Tumor Project, Genome sequencing of SHH medulloblastoma predicts genotype-related response to smoothened inhibition., *Cancer Cell* **25**, 393–405 (2014).

11. C. Hui, S. Angers, Gli Proteins in Development and Disease, *Annu. Rev. Cell Dev. Biol.* **27**, 513–537 (2011).

12. B. Wang, J. F. Fallon, P. A. Beachy, Hedgehog-regulated processing of Gli3 produces an anterior/posterior repressor gradient in the developing vertebrate limb., *Cell* **100**, 423–34 (2000).

13. D. Tempé, M. Casas, S. Karaz, M.-F. Blanchet-Tournier, J.-P. Concordet, Multisite protein kinase A and glycogen synthase kinase 3beta phosphorylation leads to Gli3 ubiquitination by SCFbetaTrCP., *Mol. Cell. Biol.* **26**, 4316–26 (2006).

14. Y. Pan, C. B. Bai, A. L. Joyner, B. Wang, Sonic hedgehog Signaling Regulates Gli2 Transcriptional Activity by Suppressing Its Processing and Degradation, *Mol. Cell. Biol.* **26**, 3365–3377 (2006).

15. D. J. Robbins, D. L. Fei, N. A. Riobo, The hedgehog signal transduction network, *Sci Signal* **5**, re6 (2012).

16. A. K. Dubey, S. Dubey, S. S. Handu, M. A. Qazi, Vismodegib: the first drug approved for advanced and metastatic basal cell carcinoma., *J. Postgrad. Med.* **59**, 48–50 (2013).

17. H. J. Sharpe, G. Pau, G. J. Dijkgraaf, N. Basset-Seguin, Z. Modrusan, T. Januario, V. Tsui, A. B. Durham, A. a Dlugosz, P. M. Haverty, R. Bourgon, J. Y. Tang, K. Y. Sarin, L. Dirix, D. C. Fisher, C. M. Rudin, H. Sofen, M. R. Migden, R. L. Yauch, F. J. de Sauvage, Genomic analysis of smoothened inhibitor resistance in Basal cell carcinoma., *Cancer Cell* **27**, 327–41 (2015).

18. A. Gajjar, C. F. Stewart, D. W. Ellison, S. Kaste, L. E. Kun, R. J. Packer, S. Goldman, M. Chintagumpala, D. Wallace, N. Takebe, J. M. Boyett, R. J. Gilbertson, T. Curran, Phase I Study of Vismodegib in Children with Recurrent or Refractory Medulloblastoma: A Pediatric Brain

Tumor Consortium Study, *Clin. Cancer Res.* **19**, 6305–6312 (2013).

19. G. W. Robinson, B. A. Orr, G. Wu, S. Gururangan, T. Lin, I. Qaddoumi, R. J. Packer, S. Goldman, M. D. Prados, A. Desjardins, M. Chintagumpala, N. Takebe, S. C. Kaste, M. Rusch, S. J. Allen, A. Onar-Thomas, C. F. Stewart, M. Fouladi, J. M. Boyett, R. J. Gilbertson, T. Curran, D. W. Ellison, A. Gajjar, Vismodegib Exerts Targeted Efficacy Against Recurrent Sonic Hedgehog-Subgroup Medulloblastoma: Results From Phase II Pediatric Brain Tumor Consortium Studies PBTC-025B and PBTC-032., *J. Clin. Oncol.* **33**, 2646–54 (2015).

20. C. M. Rudin, C. L. Hann, J. Laterra, R. L. Yauch, C. a Callahan, L. Fu, T. Holcomb, J. Stinson, S. E. Gould, B. Coleman, P. M. LoRusso, D. D. Von Hoff, F. J. de Sauvage, J. a Low, Treatment of medulloblastoma with hedgehog pathway inhibitor GDC-0449., *N. Engl. J. Med.* **361**, 1173–1178 (2009).

21. B. Li, D. L. Fei, C. A. Flaveny, N. Dahmane, V. Baubet, Z. Wang, F. Bai, X.-H. Pei, J. Rodriguez-Blanco, B. Hang, D. Orton, L. Han, B. Wang, A. J. Capobianco, E. Lee, D. J. Robbins, Pyrvinium Attenuates Hedgehog Signaling Downstream of Smoothened, *Cancer Res.* **74**, 4811–4821 (2014).

22. B. Li, D. Orton, L. R. Neitzel, L. Astudillo, C. Shen, J. Long, X. Chen, K. C. Kirkbride, T. Doundoulakis, M. L. Guerra, J. Zaias, D. L. Fei, J. Rodriguez-Blanco, C. Thorne, Z. Wang, K. Jin, D. M. Nguyen, L. R. Sands, F. Marchetti, M. T. Abreu, M. H. Cobb, A. J. Capobianco, E. Lee, D. J. Robbins, Differential abundance of CK1α provides selectivity for pharmacological CK1α activators to target WNT-dependent tumors., *Sci. Signal.* **10**, eaak9916 (2017).

23. N. Zhukova, V. Ramaswamy, M. Remke, E. Pfaff, D. J. H. Shih, D. C. Martin, P. Castelo-Branco, B. Baskin, P. N. Ray, E. Bouffet, A. O. von Bueren, D. T. W. Jones, P. A. Northcott, M. Kool, D. Sturm, T. J. Pugh, S. L. Pomeroy, Y.-J. Cho, T. Pietsch, M. Gessi, S. Rutkowski, L. Bognar, A. Klekner, B.-K. Cho, S.-K. Kim, K.-C. Wang, C. G. Eberhart, M. Fevre-Montange, M. Fouladi, P. J. French, M. Kros, W. A. Grajkowska, N. Gupta, W. A. Weiss, P. Hauser, N. Jabado, A. Jouvet, S. Jung, T. Kumabe, B. Lach, J. R. Leonard, J. B. Rubin, L. M. Liau, L. Massimi, I. F. Pollack, Y. Shin Ra, E. G. Van Meir, K. Zitterbart, U. Schüller, R. M. Hill, J. C.

Lindsey, E. C. Schwalbe, S. Bailey, D. W. Ellison, C. Hawkins, D. Malkin, S. C. Clifford, A. Korshunov, S. Pfister, M. D. Taylor, U. Tabori, Subgroup-specific prognostic implications of TP53 mutation in medulloblastoma., *J. Clin. Oncol.* **31**, 2927–35 (2013).

24. V. Ramaswamy, C. Nör, M. D. Taylor, p53 and Medulloblastoma, *Cold Spring Harb. Perspect. Med.* **6**, a026278 (2016).

25. D. L. Fei, H. Li, C. D. Kozul, K. E. Black, S. Singh, J. A. Gosse, J. DiRenzo, K. A. Martin, B. Wang, J. W. Hamilton, M. R. Karagas, D. J. Robbins, Activation of Hedgehog signaling by the environmental toxicant arsenic may contribute to the etiology of arsenic-induced tumors., *Cancer Res.* **70**, 1981–8 (2010).

26. X. Zhao, T. Ponomaryov, K. J. Ornell, P. Zhou, S. K. Dabral, E. Pak, W. Li, S. X. Atwood, R. J. Whitson, A. L. S. Chang, J. Li, A. E. Oro, J. A. Chan, J. F. Kelleher, R. A. Segal, RAS/MAPK Activation Drives Resistance to Smo Inhibition, Metastasis, and Tumor Evolution in Shh Pathway-Dependent Tumors., *Cancer Res.* **75**, 3623–35 (2015).

27. H. Y. Lee, L. A. Greene, C. A. Mason, M. C. Manzini, Isolation and culture of post-natal mouse cerebellar granule neuron progenitor cells and neurons., *J. Vis. Exp.* (2009), doi:10.3791/990.

28. J. Rodriguez-Blanco, N. S. Schilling, R. Tokhunts, C. Giambelli, J. Long, D. Liang Fei, S. Singh, K. E. Black, Z. Wang, F. Galimberti, P. A. Bejarano, S. Elliot, M. K. Glassberg, D. M. Nguyen, W. W. Lockwood, W. L. Lam, E. Dmitrovsky, A. J. Capobianco, D. J. Robbins, The Hedgehog processing pathway is required for NSCLC growth and survival, *Oncogene* (2012), doi:10.1038/onc.2012.243.

29. J. Rodriguez-Blanco, V. Martín, F. Herrera, G. García-Santos, I. Antolín, C. Rodriguez, Intracellular signaling pathways involved in post-mitotic dopaminergic PC12 cell death induced by 6-hydroxydopamine., *J. Neurochem.* **107**, 127–40 (2008).

30. L. V Goodrich, L. Milenković, K. M. Higgins, M. P. Scott, Altered neural cell fates and medulloblastoma in mouse patched mutants., *Science* **277**, 1109–13 (1997).

31. J. Rodriguez-Blanco, L. Pednekar, C. Penas, B. Li, V. Martin, J. Long, E. Lee, W. A. Weiss,

C. Rodriguez, N. Mehrdad, D. M. Nguyen, N. G. Ayad, P. Rai, A. J. Capobianco, D. J. Robbins, Inhibition of WNT signaling attenuates self-renewal of SHH-subgroup medulloblastoma., *Oncogene* **36**, 6306–6314 (2017).

32. R. J. Ward, L. Lee, K. Graham, T. Satkunendran, K. Yoshikawa, E. Ling, L. Harper, R. Austin, E. Nieuwenhuis, I. D. Clarke, C. Hui, P. B. Dirks, Multipotent CD15 + Cancer Stem Cells in Patched-1 – Deficient Mouse Medulloblastoma, *Cancer Res.* , 4682–4690 (2009).

33. X. Huang, T. Ketova, Y. Litingtung, C. Chiang, Isolation, enrichment, and maintenance of medulloblastoma stem cells., *J. Vis. Exp.* (2010), doi:10.3791/2086.

34. S. K. Singh, C. Hawkins, I. D. Clarke, J. A. Squire, J. Bayani, T. Hide, R. M. Henkelman, M. D. Cusimano, P. B. Dirks, Identification of human brain tumour initiating cells, *Nature* **432**, 396–401 (2004).

35. S. K. Singh, I. D. Clarke, M. Terasaki, V. E. Bonn, C. Hawkins, J. Squire, P. B. Dirks, Identification of a cancer stem cell in human brain tumors., *Cancer Res.* **63**, 5821–8 (2003).

36. R. J. Vanner, M. Remke, M. Gallo, H. J. Selvadurai, F. Coutinho, L. Lee, M. Kushida, R. Head, S. Morrissy, X. Zhu, T. Aviv, V. Voisin, I. D. Clarke, Y. Li, A. J. Mungall, R. A. Moore, Y. Ma, S. J. M. Jones, M. A. Marra, D. Malkin, P. A. Northcott, M. Kool, S. M. Pfister, G. Bader, K. Hochedlinger, A. Korshunov, M. D. Taylor, P. B. Dirks, Quiescent sox2(+) cells drive hierarchical growth and relapse in sonic hedgehog subgroup medulloblastoma., *Cancer Cell* **26**, 33–47 (2014).

37. D. Corno, M. Pala, M. Cominelli, B. Cipelletti, K. Leto, L. Croci, V. Barili, F. Brandalise, R. Melzi, A. Di Gregorio, L. S. Sergi, L. S. Politi, L. Piemonti, A. Bulfone, P. Rossi, F. Rossi, G. G. Consalez, P. L. Poliani, R. Galli, Gene Signatures Associated with Mouse Postnatal Hindbrain Neural Stem Cells and Medulloblastoma Cancer Stem Cells Identify Novel Molecular Mediators and Predict Human Medulloblastoma Molecular Classification, *Cancer Discov.* **2**, 554–568 (2012).

38. K. Sasai, J. T. Romer, Y. Lee, D. Finkelstein, C. Fuller, P. J. McKinnon, T. Curran, Shh pathway activity is down-regulated in cultured medulloblastoma cells: implications for preclinical

studies, *Cancer Res* **66**, 4215–4222 (2006).

39. T. C. Smith, A. W. Kinkel, C. M. Gryczko, J. R. Goulet, Absorption of pyrvinium pamoate., *Clin. Pharmacol. Ther.* **19**, 802–6 (1976).

40. B. A. Hatton, E. H. Villavicencio, K. D. Tsuchiya, J. I. Pritchard, S. Ditzler, B. Pullar, S. Hansen, S. E. Knoblaugh, D. Lee, C. G. Eberhart, A. R. Hallahan, J. M. Olson, The Smo/Smo model: hedgehog-induced medulloblastoma with 90% incidence and leptomeningeal spread., *Cancer Res.* **68**, 1768–76 (2008).

41. B. a Hatton, E. H. Villavicencio, J. Pritchard, M. LeBlanc, S. Hansen, M. Ulrich, S. Ditzler, B. Pullar, M. R. Stroud, J. M. Olson, Notch signaling is not essential in sonic hedgehog-activated medulloblastoma., *Oncogene* **29**, 3865–3872 (2010).

42. J. Yang, W. Huang, W. Tan, Solasonine, A Natural Glycoalkaloid Compound, Inhibits Gli-Mediated Transcriptional Activity, *Molecules* **21**, 1364 (2016).

43. S. Pricl, B. Cortelazzi, V. Dal Col, D. Marson, E. Laurini, M. Fermeglia, L. Licitra, S. Pilotti, P. Bossi, F. Perrone, Smoothened (SMO) receptor mutations dictate resistance to vismodegib in basal cell carcinoma., *Mol. Oncol.* **9**, 389–97 (2015).

44. D. N. Louis, A. Perry, G. Reifenberger, A. von Deimling, D. Figarella-Branger, W. K. Cavenee, H. Ohgaki, O. D. Wiestler, P. Kleihues, D. W. Ellison, The 2016 World Health Organization Classification of Tumors of the Central Nervous System: a summary, *Acta Neuropathol.* **131**, 803–820 (2016).

45. S. X. Atwood, K. Y. Sarin, R. J. Whitson, J. R. Li, G. Kim, M. Rezaee, M. S. Ally, J. Kim, C. Yao, A. L. S. Chang, A. E. Oro, J. Y. Tang, Smoothened variants explain the majority of drug resistance in Basal cell carcinoma., *Cancer Cell* **27**, 342–53 (2015).

46. C. A. Thorne, A. J. Hanson, J. Schneider, E. Tahinci, D. Orton, C. S. Cselenyi, K. K. Jernigan, K. C. Meyers, B. I. Hang, A. G. Waterson, K. Kim, B. Melancon, V. P. Ghidu, G. A. Sulikowski, B. LaFleur, A. Salic, L. A. Lee, D. M. Miller, E. Lee, Small-molecule inhibition of Wnt signaling through activation of casein kinase 1α, *Nat. Chem. Biol.* **6**, 829–836 (2010).

47. V. Ramaswamy, M. D. Taylor, Medulloblastoma: From Myth to Molecular., *J. Clin. Oncol.*

35, 2355–2363 (2017).

48. L. Garzia, N. Kijima, A. S. Morrissy, P. De Antonellis, A. Guerreiro-Stucklin, B. L. Holgado, X. Wu, X. Wang, M. Parsons, K. Zayne, A. Manno, C. Kuzan-Fischer, C. Nor, L. K. Donovan, J. Liu, L. Qin, A. Garancher, K.-W. Liu, S. Mansouri, B. Luu, Y. Y. Thompson, V. Ramaswamy, J. Peacock, H. Farooq, P. Skowron, D. J. H. Shih, A. Li, S. Ensan, C. S. Robbins, M. Cybulsky, S. Mitra, Y. Ma, R. Moore, A. Mungall, Y.-J. Cho, W. A. Weiss, J. A. Chan, C. E. Hawkins, M. Massimino, N. Jabado, M. Zapotocky, D. Sumerauer, E. Bouffet, P. Dirks, U. Tabori, P. H. B. Sorensen, P. K. Brastianos, K. Aldape, S. J. M. Jones, M. A. Marra, J. R. Woodgett, R. J. Wechsler-Reya, D. W. Fults, M. D. Taylor, A Hematogenous Route for Medulloblastoma Leptomeningeal Metastases., *Cell* **172**, 1050–1062.e14 (2018).

49. S. T. Lee, K. D. Welch, K. E. Panter, D. R. Gardner, M. Garrossian, C.-W. T. Chang, Cyclopamine: From Cyclops Lambs to Cancer Treatment, *J. Agric. Food Chem.* **62**, 7355–7362 (2014).

50. T. Rimkus, R. Carpenter, S. Qasem, M. Chan, H.-W. Lo, Targeting the Sonic Hedgehog Signaling Pathway: Review of Smoothened and GLI Inhibitors, *Cancers (Basel).* **8**, 22 (2016).

51. S. Pricl, B. Cortelazzi, V. Dal Col, D. Marson, E. Laurini, M. Fermeglia, L. Licitra, S. Pilotti, P. Bossi, F. Perrone, Smoothened (SMO) receptor mutations dictate resistance to vismodegib in basal cell carcinoma, *Mol. Oncol.* **9**, 389–397 (2015).

52. S. X. Atwood, R. J. Whitson, A. E. Oro, Advanced treatment for basal cell carcinomas., *Cold Spring Harb. Perspect. Med.* **4**, a013581 (2014).

53. A. S. Bhagwat, C. R. Vakoc, Targeting Transcription Factors in Cancer., *Trends in cancer* **1**, 53–65 (2015).

54. J. Kim, J. J. Lee, J. Kim, D. Gardner, P. A. Beachy, Arsenic antagonizes the Hedgehog pathway by preventing ciliary accumulation and reducing stability of the Gli2 transcriptional effector, *Proc. Natl. Acad. Sci.* **107**, 13432–13437 (2010).

55. K. H. Antman, Introduction: the history of arsenic trioxide in cancer therapy., *Oncologist* **6 Suppl 2**, 1–2 (2001).

56. W.-Y. Au, S. Tam, B. M. Fong, Y.-L. Kwong, Determinants of cerebrospinal fluid arsenic concentration in patients with acute promyelocytic leukemia on oral arsenic trioxide therapy, *Blood* **112**, 3587–3590 (2008).

57. Y. Zhao, C.-Y. Yang, S. Wang, The Making of I-BET762, a BET Bromodomain Inhibitor Now in Clinical Development, *J. Med. Chem.* **56**, 7498–7500 (2013).

58. Y. Tang, S. Gholamin, S. Schubert, M. I. Willardson, A. Lee, P. Bandopadhayay, G. Bergthold, S. Masoud, B. Nguyen, N. Vue, B. Balansay, F. Yu, S. Oh, P. Woo, S. Chen, A. Ponnuswami, M. Monje, S. X. Atwood, R. J. Whitson, S. Mitra, S. H. Cheshier, J. Qi, R. Beroukhim, J. Y. Tang, R. Wechsler-Reya, A. E. Oro, B. A. Link, J. E. Bradner, Y.-J. Cho, Epigenetic targeting of Hedgehog pathway transcriptional output through BET bromodomain inhibition, *Nat. Med.* **20**, 732–740 (2014).

59. J. Long, B. Li, J. Rodriguez-Blanco, C. Pastori, C.-H. Volmar, C. Wahlestedt, A. Capobianco, F. Bai, X.-H. Pei, N. G. Ayad, D. J. Robbins, The BET bromodomain inhibitor I-BET151 acts downstream of smoothened protein to abrogate the growth of hedgehog protein-driven cancers., *J. Biol. Chem.* **289**, 35494–502 (2014).

60. A. Ruiz i Altaba, Hedgehog signaling and the Gli code in stem cells, cancer, and metastases., *Sci. Signal.* **4**, pt9 (2011).

61. B. Li, C. A. Flaveny, C. Giambelli, D. L. Fei, L. Han, B. I. Hang, F. Bai, X.-H. Pei, V. Nose, O. Burlingame, A. J. Capobianco, D. Orton, E. Lee, D. J. Robbins, Repurposing the FDA-approved pinworm drug pyrvinium as a novel chemotherapeutic agent for intestinal polyposis., *PLoS One* **9**, e101969 (2014).

Figure 1: SSTC3 acts downstream of SMO to attenuate SHH activity. **A**. Light2 cells were treated with 1 μg/ml recombinant SHH for 24 h, followed by addition of the indicated concentrations of SSTC3 or SSTC111 for an additional 48 h. Firefly luciferase activity was then determined and normalized to renilla luciferase activity. **B**. NIH-3T3 cells were incubated with the SMO agonist SAG (100 nM) and the indicated concentrations of SSTC3. The expression of *GLI1* was determined at the indicated time points and normalized to that of the housekeeping gene *GAPDH*. **C**. Light2 cells were transduced with lentivirus expressing the indicated shRNA to generate stable polyclonal cell lines. These cells were treated with SAG (100 nM) and SSTC3 (200 nM) for 48 h. The expression of *GLI1* was determined and normalized to that of *GAPDH*. **D**. Granular Precursor Cells (GPC) were incubated in the presence of DMSO, SAG (100 nM), or SAG (100 nM) and SSTC3 (200 nM), for 24 h prior to quantification of BrdU incorporation. **E**. Representative images from similarly treated GPC are shown. **F**. GPC were treated with vehicle, SAG (100 nM) and SSTC3 (200 nM) or vismodegib (100 nM), and expression of the indicated genes determined 6 h later. **G**. $Sufu^{-/-}$ MEFs were treated for 48 h with vehicle, the indicated concentrations of SSTC3, or vismodegib (200 nM). The expression of *GLI1* was then determined and normalized to that of *GAPDH*. **H**. Light2 cells expressing wild type (WT) *SMO*, the vismodegib resistant oncogenic *SMO* mutant *M2-D473* or *GLI1,* were treated with vehicle, vismodegib (200 nM) or SSTC3 (200 nM). Firefly luciferase activity was then determined and normalized to renilla luciferase activity. **I**. NIH-3T3 cells expressing epitope *MYC*-tagged *GLI1* were treated with 100 μg/ml cycloheximide (CHX) at the indicated time points, in the presence of pyrvinium (100 nM), SSTC3 (200 nM) or vehicle control. GLI1, and GAPDH, levels were determined by immunoblotting.

Supplemental 1: ***CK1α*** **knockdown decreases CK1α protein levels.** Light2 cells were transduced with lentivirus expressing the indicated shRNA to generate stable polyclonal lines. The levels of the indicated proteins were determined by immunoblotting with antisera to CK1α or TUBULIN.

Figure 2: SSTC3 inhibits the growth of SHH subgroup medulloblastoma. A. Medulloblastoma sphere cultures (MSC) were isolated from a $PTCH1^{+/-}$ MB. The MSC were incubated for 3 days with the indicated concentrations of vismodegib and cell viability determined using a MTT reduction assay. **B**. *PTCH1* mutant MSC were transduced with the indicated *shRNA* and cell viability determined 5 days later using a MTT assay. **C.** *GLI1* expression determined in similarly transduced cells 3 days after infection. **D.** *PTCH1* mutant MSC were treated with the indicated concentrations of SSTC3 or SSTC111, and cell viability determined 3 days later. **E.** Expression of the indicated genes in similarly treated cells was determined 24 h after treatment. **F**. *PTCH1* mutant MSC were treated with the indicated concentrations of SSTC3 and proliferation determined by BrdU incorporation 24 h later. **G**. Mice carrying orthotopically implanted *PTCH1* mutant MB tumors were treated every other day with SSTC3 (10 mg/kg) or vehicle for 30 days. The mice were then sacrificed, their brains harvested and the size of the residual tumors determined. **H**. The residual tumors from these mice were immunostained for the proliferation biomarker PCNA and the numbers of $PCNA^{+}$ cells per field quantified. **I**. Representative images of PCNA immunostained cells are shown. These residual tumors were immunostained for the apoptosis biomarker Cleaved CASPASE-3 and the numbers of Cleaved CASPASE-3^{+} cells per field quantified. **K**. Representative images of Cleaved CASPASE-3 immunostaining are shown.

Supplemental 2: SSTC3 is a blood brain barrier penetrant small-molecule capable of reducing orthotopic medulloblastoma growth. A. *PTCH1* mutant MSC were treated with the indicated concentrations of vismodegib, and the expression of the indicated genes determined 24 h later and

normalized to the expression of the housekeeping gene *GAPDH*. **B**. SSTC3 distribution was determined in mouse plasma and brain tissue at the indicated times. **C.** Mice carrying orthotopic *PTCH1* mutant MB were treated every other day with SSTC3 (10 mg/kg) or vehicle for 30 days. Representative H&E staining of residual tumors from these mice is shown. **D**. Mice carrying flank *PTCH1* mutant MB were treated for 48 h with SSTC3 (25 mg/kg) or vehicle control for 48 h. Tissues were harvested 6 h after the last injection and expression of the indicated genes determined by RT-qPCR. **E**. GLI1 levels determined by immunoblotting in similarly treated mice. NIH-3T3 cells overexpressing *GLI1* or *GLI2* were used to show antibody specificity. GLI1 levels from **E** were quantified using Image-J. **G**. *PTCH1* mutant MSC were treated with the indicated concentrations of SSTC3, and expression of the indicated genes determined 24 h later and normalized to that of the housekeeping gene *GAPDH*.

Figure 3: SSTC3 increases the symptom-free survival of a genetically engineered mouse model of SHH subgroup medulloblastoma. A. Two-month old *ND2:SMOA1* mice were treated with vehicle or SSTC3 (20 mg/kg) daily for 1 month. Representative IVIS images from vehicle or SSTC3 treated mice are shown. **B**. Similar mice were treated every other day with SSTC3 (10 mg/kg) for a month. Representative images of brains from wild type or *ND2:SMOA1* vehicle or SSTC3 treated mice are shown. **C**. Representative H&E staining of residual tumors from these mice. **D**. The area of tumor from the vehicle and SSTC3 treated mice was determined. **E**. Tumor burden, defined as the number of *in situ* and metastatic tumors per section, was quantified for these orthotopic tumors. **F**. Tumors from these mice were immunostained for the proliferation biomarker PCNA and the numbers of positive cells per field quantified. **G**. Representative images of PCNA immunostaining are shown. **H**. Orthotopic tumors were immunostained for the apoptosis biomarker Cleaved CASPASE-3 and the numbers of positive cells per field quantified. **I**. Representative images of Cleaved CASPASE-3 immunostaining are shown. **J**. Four-month old *ND2:SMOA1* mice were treated with vehicle or 10 mg/kg SSTC3 for 2 consecutive days. The mice were then sacrificed and their cerebella harvested 6 h after the last injection. The expression of the indicated genes was then determined and normalized to the expression of *GAPDH*. **K.** Two-month old *ND2:SMOA1* mice were treated with 10 mg/kg SSTC3 every other day for 1 month, and MB symptom-free survival monitored for 10 additional months.

Supplemental 3: SSTC3 promotes apoptosis without affecting WNT signaling in *SMOA1* driven medulloblastoma. A. Two-month old *ND2:SMOA1* mice were treated with 10 mg/kg SSTC3 every other day for 1 month. DNA fragmentation was determined using a TUNEL assay in tumors from the indicated mice. **B**. Representative images of TUNEL staining are shown. **C**. Four-month old *ND2:SMOA1* mice were treated with vehicle or 10 mg/kg SSTC3 for 2 consecutive days, 6 h after the last injection the mice were sacrificed and their cerebella harvested. The expression of the indicated genes was then determined and normalized to that of *GAPDH*.

Figure 4: SSTC3 inhibits the growth of a patient derived SHH subgroup medulloblastoma model. A. Mice carrying an orthotopically implanted SHH subgroup MB PDX (*TRP53* mutant, *MYCN* amplified) were treated for two consecutive days with vehicle or 10 mg/kg SSTC3. Residual tumor tissue was harvested 6 h after the last injection and expression of the indicated genes determined and normalized to that of *GAPDH*. **B**. Mice carrying an orthotopically implanted PDX, engineered to express luciferase, were treated daily with vehicle or SSTC3 (10 mg/kg) for 10 days. Tumor growth was determined by IVIS imaging on day 3 and 10. Representative IVIS imaging is shown. **C**. Mice carrying an orthotopically implanted MB PDX were treated with vehicle or SSTC3 (10 mg/kg) every other day for 30 days. The size of the tumors from these mice was then determined. **D**. Representative

H&E staining of tumors from these mice. **E**. Residual tumors from these mice were immunostained for the proliferation biomarker PCNA and the number of positive cells per field quantified. **F**. Representative images of PCNA immunostaining are shown. **G**. Residual tumors from these mice were immunostained for the apoptosis biomarker Cleaved CASPASE-3 and the numbers of positive cells per field quantified. **H**. Representative images of Cleaved CASPASE-3 immunostaining are shown. **I**. Mice carrying an orthotopically implanted MB PDX were treated with vehicle or SSTC3 (10 mg/kg) every other day for 30 days and MB symptom-free survival monitored.

Supplemental 4: SSTC3 inhibits the growth of a PDX medulloblastoma model. A. Patient derived SHH-subgroup MB cells (*TRP53* mutant, *MYCN* amplified) were orthotopically implanted into the brains of immunocompromised mice and allowed to form tumors *in vivo*: **(a)** Image of a non-symptomatic mouse. **(b)** Image of a symptomatic mouse. **(c)** Representative image of a naïve brain. **(d)** Representative image of a brain carrying this PDX. **(e)** Representative H&E staining of tumor growth in the cerebellum. **(f)** Representative image of intraventricular tumor spread. **(g)** Representative image of cerebral tumor spread. **(h)** Representative image of leptomeningeal tumor dissemination. **B**. Mice carrying an orthotopically implanted MB PDX, engineered to express *luciferase,* were treated daily with vehicle or SSTC3 (10 mg/kg) for 10 days. Tumor growth was quantitated by IVIS imaging on day 3 and 10 post-implantation (5 mice per group). **C.** Mice carrying an orthotopically implanted MB PDX were treated daily with vehicle or SSTC3 (10 mg/kg) every other day for 30 days. DNA fragmentation was determined in tumors using a TUNEL assay. **D**. Representative images of TUNEL staining are shown. **E**. Mice carrying an orthotopically implanted MB PDX were treated for two consecutive days with vehicle or 10 mg/kg SSTC3. Tumor tissue was harvested 6 h after the last injection and expression of the indicated genes determined and normalized to that of *GAPDH*.

Figure 1

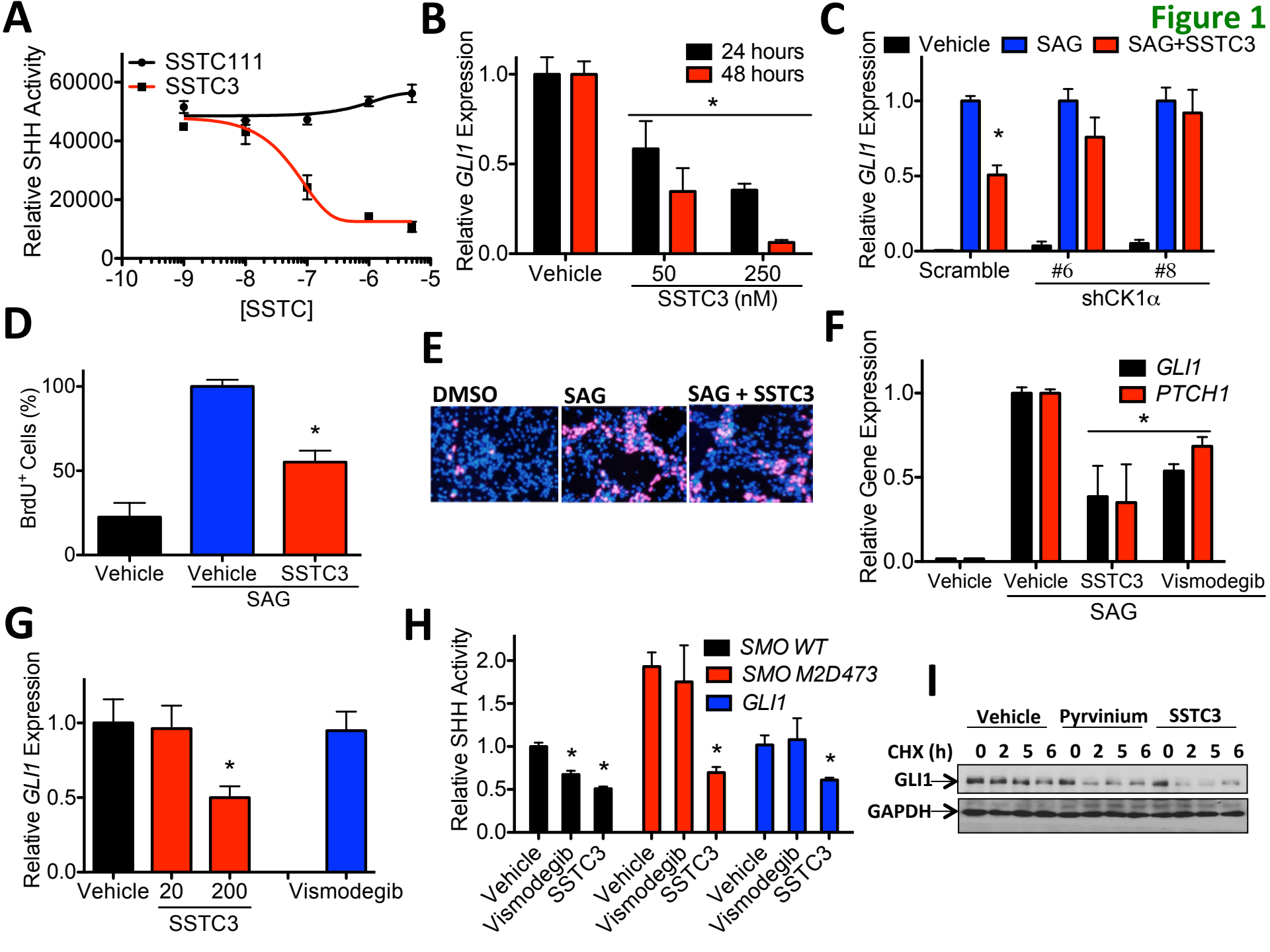
A
Relative SHH Activity
SSTC111
SSTC3
60000
40000
20000
0
-10
-9
-8
-7
-6
-5
[SSTC]
B
Relative GLI1 Expression
24 hours
48 hours
1.0
0.5
0.0
*
Vehicle
50
250
SSTC3 (nM)
C
Relative GLI1 Expression
Vehicle
SAG
SAG+SSTC3
1.0
0.5
0.0
*
Scramble
#6
#8
shCK1α
D
BrdU+ Cells (%)
100
50
0
*
Vehicle
Vehicle
SSTC3
SAG
E
DMSO
SAG
SAG + SSTC3
F
Relative Gene Expression
GLI1
PTCH1
1.0
0.5
0.0
*
Vehicle
Vehicle
SSTC3
Vismodegib
SAG
G
Relative GLI1 Expression
1.0
0.5
0.0
*
Vehicle
20
200
SSTC3
Vismodegib
H
Relative SHH Activity
SMO WT
SMO M2D473
GLI1
2.0
1.5
1.0
0.5
0.0
*
*
*
*
Vehicle
Vismodegib
SSTC3
Vehicle
Vismodegib
SSTC3
Vehicle
Vismodegib
SSTC3
I
Vehicle
Pyrvinium
SSTC3
CHX (h)
0 2 5 6 0 2 5 6 0 2 5 6
GLI1
GAPDH

Supplemental 1

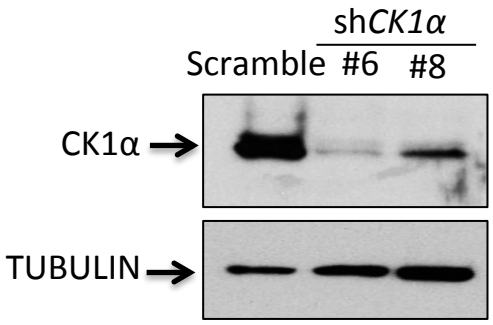

Figure 2

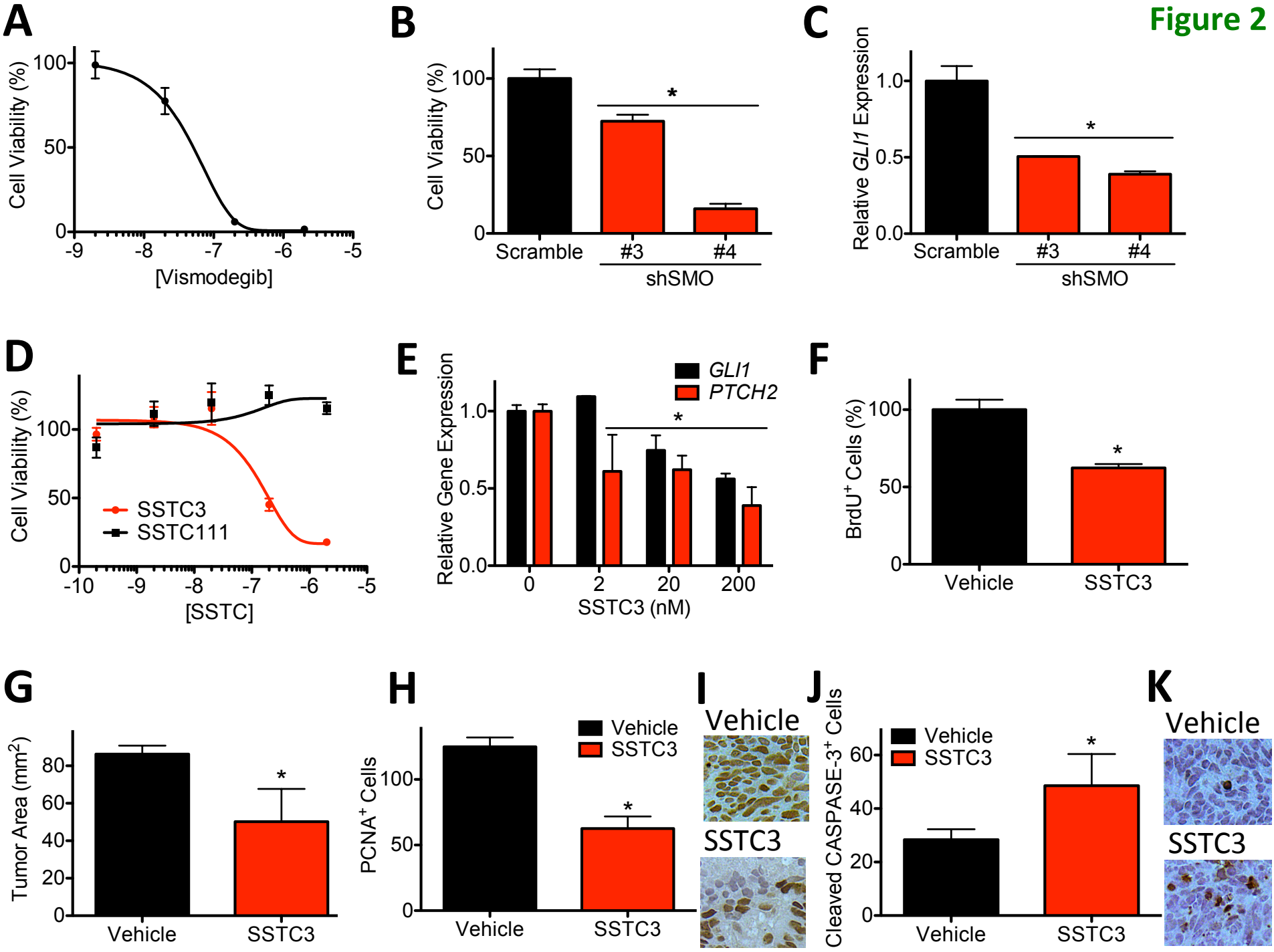
A
Cell Viability (%)
100
50
0
-9
-8
-7
-6
-5
[Vismodegib]
B
Cell Viability (%)
100
50
0
*
Scramble
#3
#4
shSMO
C
Relative GLI1 Expression
1.0
0.5
0.0
*
Scramble
#3
#4
shSMO
D
Cell Viability (%)
100
50
0
SSTC3
SSTC111
-10
-9
-8
-7
-6
-5
[SSTC]
E
Relative Gene Expression
1.0
0.5
0.0
GLI1
PTCH2
*
0
2
20
200
SSTC3 (nM)
F
BrdU+ Cells (%)
100
50
0
*
Vehicle
SSTC3
G
Tumor Area (mm2)
80
60
40
20
0
*
Vehicle
SSTC3
H
PCNA+ Cells
100
50
0
Vehicle
SSTC3
*
Vehicle
SSTC3
I
Vehicle
SSTC3
J
Cleaved CASPASE-3+ Cells
60
40
20
0
Vehicle
SSTC3
*
Vehicle
SSTC3
K
Vehicle
SSTC3

Supplemental 2

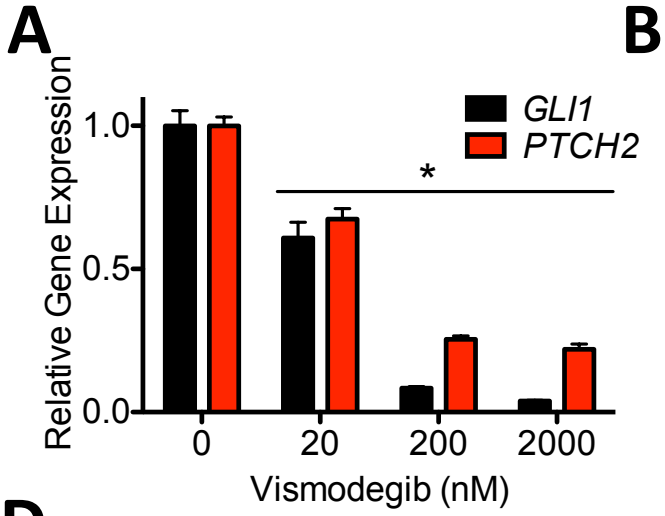

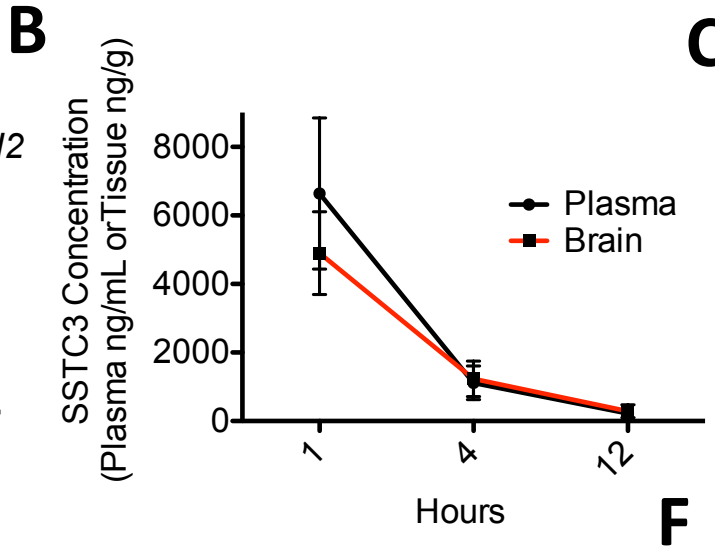

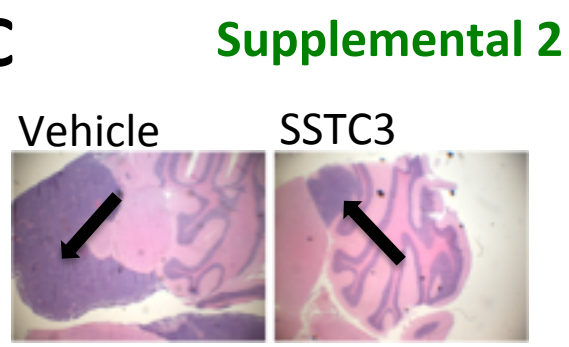

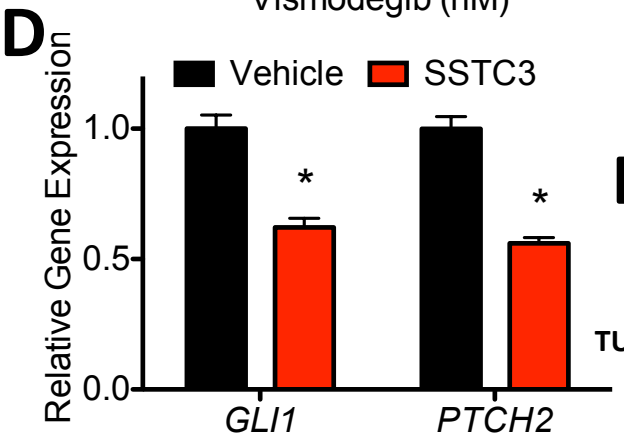

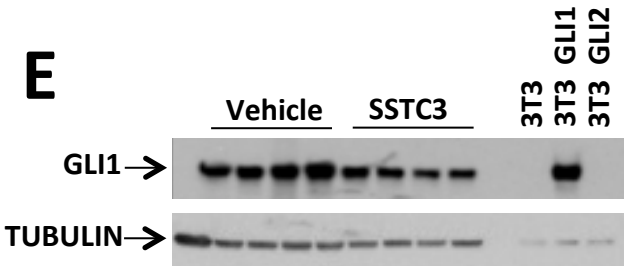

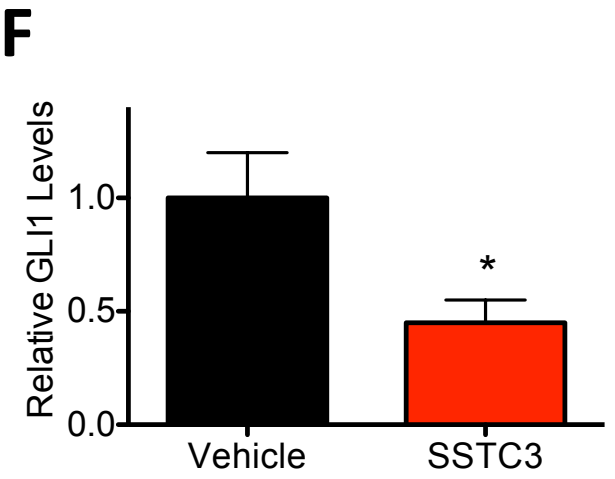

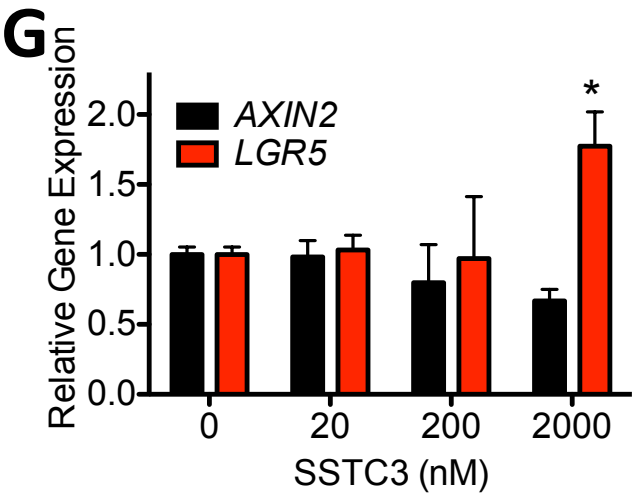

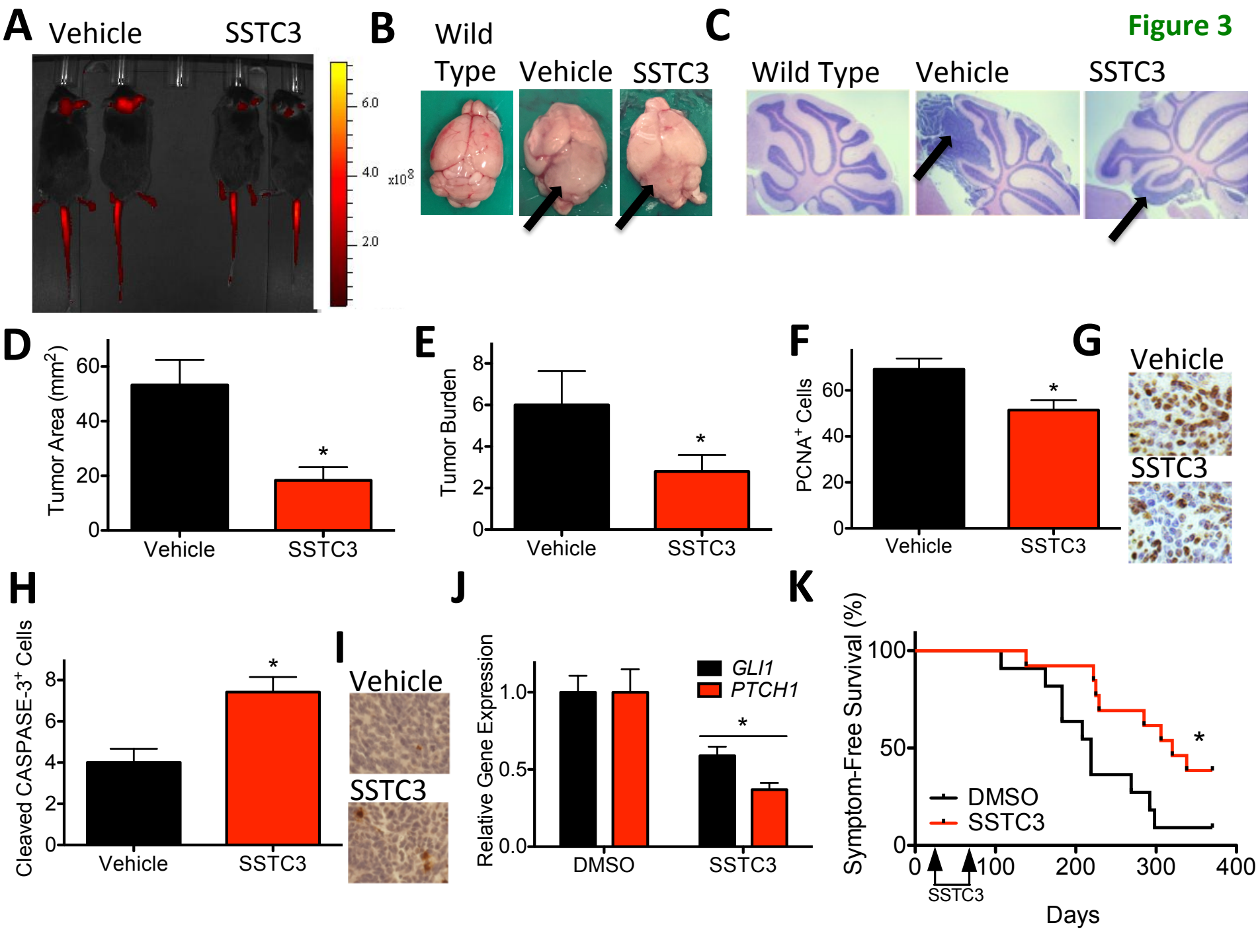
A
Vehicle
SSTC3
6.0
4.0
x10^8
2.0
B
Wild Type
Vehicle
SSTC3
C
Wild Type
Vehicle
SSTC3
D
Tumor Area (mm^2)
60
40
20
0
*
Vehicle
SSTC3
E
Tumor Burden
8
6
4
2
0
*
Vehicle
SSTC3
F
PCNA+ Cells
60
40
20
0
*
Vehicle
SSTC3
G
Vehicle
SSTC3
H
Cleaved CASPASE-3+ Cells
8
6
4
2
0
*
Vehicle
SSTC3
I
Vehicle
SSTC3
J
Relative Gene Expression
1.0
0.5
0.0
GLI1
PTCH1
*
DMSO
SSTC3
K
Symptom-Free Survival (%)
100
50
0
*
DMSO
SSTC3
0
100
200
300
400
SSTC3
Days

Supplemental 3

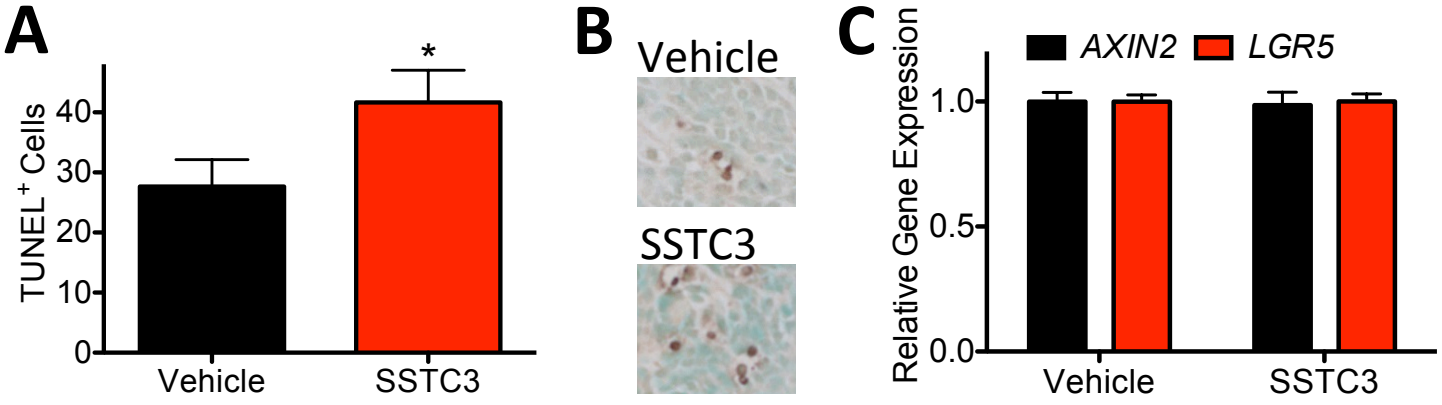

Figure 4

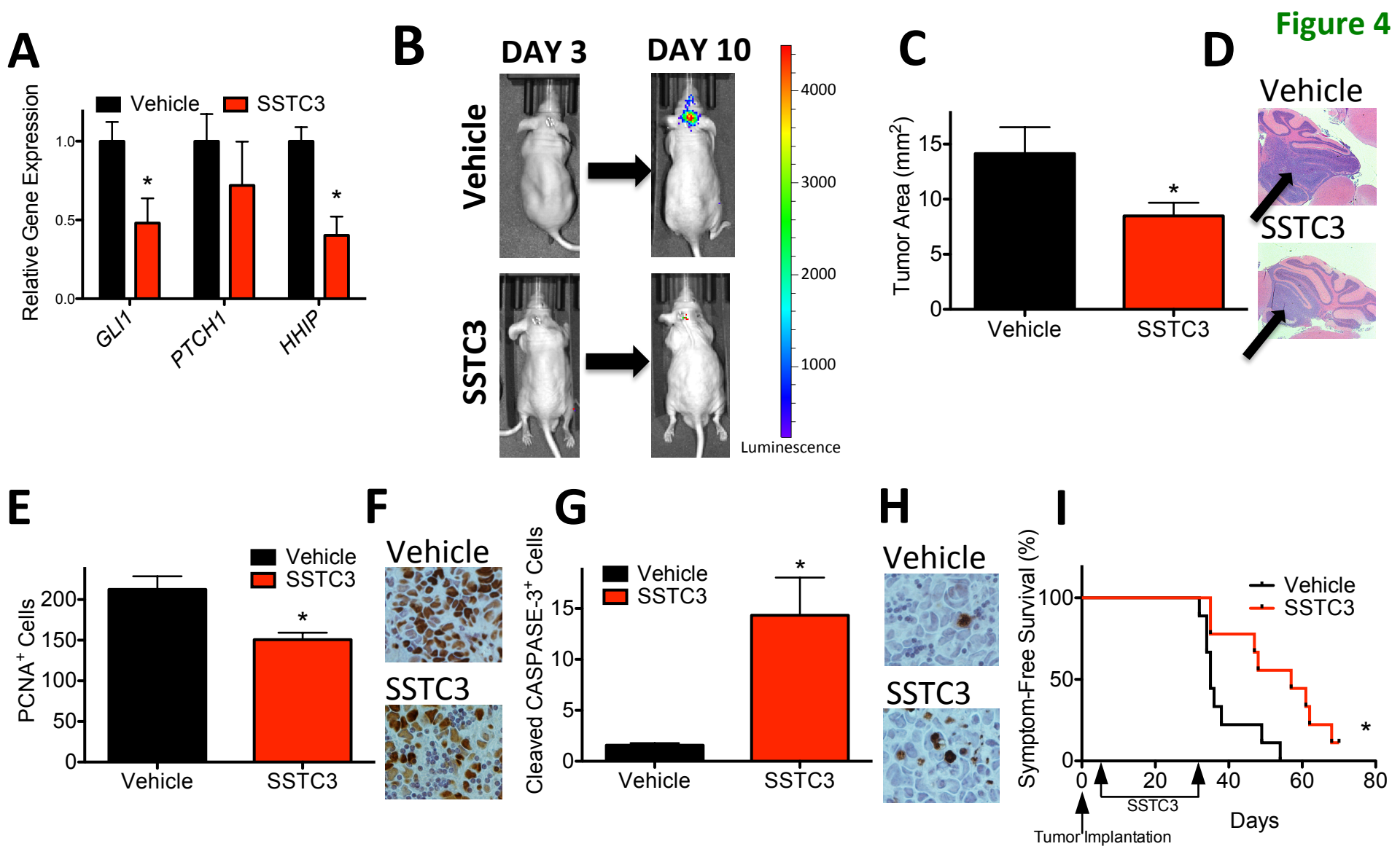
A
Relative Gene Expression
Vehicle
SSTC3
1.0
0.5
0.0
*
*
GLI1
PTCH1
HHIP
B
DAY 3
DAY 10
Vehicle
SSTC3
4000
3000
2000
1000
Luminescence
C
Tumor Area (mm2)
15
10
5
0
*
Vehicle
SSTC3
D
Vehicle
SSTC3
E
PCNA+ Cells
Vehicle
SSTC3
200
150
100
50
0
*
Vehicle
SSTC3
F
Vehicle
SSTC3
G
Cleaved CASPASE-3+ Cells
Vehicle
SSTC3
15
10
5
0
*
Vehicle
SSTC3
H
Vehicle
SSTC3
I
Symptom-Free Survival (%)
Vehicle
SSTC3
100
50
0
*
0
20
40
60
80
SSTC3
Days
Tumor Implantation

Supplemental 4